Gain-Scheduled Composite Nonlinear Feedback Control of an Exothermic Chemical Reactor*

V.-P. Pyrhonen, *Student Member, IEEE*, H.J. Koivisto

***Abstract*— This paper studies gain-scheduled composite nonlinear feedback (CNF) control of a continuous stirred tank reactor (CSTR). Inside the reactor, an exothermic chemical reaction occurs, which is commanded from high to low residual concentration. During the transition, the reaction dynamics change through stable-unstable-stable chain while the residual concentration decreases. Therefore, appropriate cooling is necessary to stabilize the reaction, and to prevent a thermal runaway and overheating of the CSTR. A full-state gain-scheduled CNF controller is designed for adjusting the coolant temperature of the CSTR. A traditional gain-scheduled cascade controller and a gain-scheduled model predictive controller (MPC) are also fabricated for comparison. The simulation results show that the closed-loop system using CNF controller is able to offer the best tracking performance as measured by the integral-of-absolute-error (IAE) criterion. In addition, the CNF controller needs fewer scheduled tuning parameters as opposed to the cascade structure.**

I. Introduction

A composite nonlinear feedback (CNF) control has been developed to satisfy simultaneous requirements on command following and robustness using constrained control. Generally, a CNF controller consists of mutually collaborating linear and nonlinear parts, which are designed as follows. First, a linear feedback part is designed for sufficient transient speed, e.g., small closed-loop damping ratio. Then, a nonlinear feedback part is attached to the control law in order to provide control error dependent damping when the output reaches the desired reference. By such mechanism, the nonlinear part is able to smoothly change the locations of closed-loop poles without any switching elements in the control structure. Therefore, the CNF controller alters the closed-loop dynamics as desired, which effectively improves the tracking performance.

The CNF originates from the work of Lin *et al.* in [1]. Since the initiation, research has been active in the field. For example, Turner *et al.* generalized CNF control for multivariable systems in [2]. Foundations for measurement feedback were laid by Chen *et al.* in [3], which was further generalized by He *et al.* in [4]. Lan *et al.* investigated the CNF for a class of nonlinear systems in [5]. Discrete time CNF was reported in [6], respectively. Lan *et al.* have also proposed a scaled nonlinear function to achieve robust transient performance as regards to variation of step amplitude in [7]. Cheng *et al.* have generalized the CNF for tracking non-step references in [8]. In [9], Pyrhonen provided conditions for generalizing the CNF using arbitrary order set point filters. Recently, composite nonlinear feedback has been applied to unmanned aerial vehicles [10], industrial robotics [8], hard disk drives [11], DC-servo motors [12–13], gantry crane systems [14], voltage source inverters [15], and water level control of a nuclear U-tube steam generator [16], amongst others.

The motivation of our study is two-fold. Firstly, we consider the suitability of CNF control within the well-known gain-scheduling framework. We would like to note that we are not aware of any previous studies which attempt to combine gain-scheduling and CNF. Secondly, we test a gain-scheduled CNF for a nonlinear process; namely, a continuous stirred tank reactor (CSTR) found in an open literature.

The CSTR process considered in this paper is an exothermic chemical reaction transitioning from low to high conversion rate, i.e. from high to low residual concentration. During such transition, the reaction liberates heat, and hence, appropriate cooling is necessary in order to stabilize the reaction and to prevent thermal runaway. Cooling is provided by adjusting the coolant temperature inside the reactor's cooling jacket. The reaction dynamics are nonlinear with strong coupling between the reactor temperature and residual concentration. Furthermore, the reaction dynamics change from stable to unstable and back to stable while the conversion rate increases. Such characteristics require, e.g. gain-scheduling or model predictive control (MPC) in order to successfully control the reaction temperature.

In this paper, we design a full-state linearization-based gain-scheduled CNF controller for adjusting the coolant temperature of the CSTR. We compare our design with a traditional gain-scheduled cascade controller using a PI-controller as the primary loop controller, whereas the secondary loop is a phase-lead compensator. We also compare our design with a gain-scheduled MPC. It should be noted that the cascade controller and MPC can both be found in MathWorks MatLab documentation: [17–18].

The tracking performances of all control systems are measured using the integral-of-absolute-error (IAE) criterion. It turns out that the closed-loop system using gain-scheduled CNF provides the best tracking performance.

The material of this paper is organized as follows. In Section 2, the mathematical model of the CSTR is introduced along with the testing environment. In Section 3, gain-scheduled cascade, MPC, and CNF controllers are presented for adjusting the coolant temperature of the CSTR. Finally, concluding remarks and suggestions for future research are presented in Section 4, respectively.

*Research supported by Walter Ahlström Foundation.

V.-P. Pyrhonen is with the Department of Automation Science and Engineering, Tampere University of Technology, P.O. Box 692, FI-33720 Tampere, Finland. (phone: +358-40-192 8348; e-mail: veli-pekka. pyrhonen@tut.fi).

H. J. Koivisto is with the Department of Automation Science and Engineering, Tampere University of Technology, P.O. Box 692, FI-33720 Tampere, Finland. (e-mail: hannu.koivisto@tut.fi).

II. Continuous Stirred Tank Reactor Model

In this paper, we consider a single-phase irreversible exothermic reaction, where chemical species A reacts to form species B. The rate of reaction is assumed to be of first order, and it obeys the Arrhenius relation. Please refer to [19] for more detailed discussion of the mathematical modelling of the CSTR. A schematic diagram of the CSTR is depicted in Fig. 1, respectively.

We assume perfect mixing inside the reactor. Therefore, the residual concentration $c_A(t)$ of the reactant A and the reactor temperature $T(t)$ are homogenously distributed inside the reactor and in the outflow piping. The flow rate F through the tank is kept constant, and hence, the liquid volume V remains constant. Following the procedures presented in [19], the CSTR can be modelled by the nonlinear differential equations

$$\begin{cases} \dfrac{d}{dt}T(t) = \dfrac{F}{V}\big(T_i(t) - T(t)\big) + \dfrac{UA}{\rho VC}\big(T_c(t) - T(t)\big) \\ \qquad\qquad + \dfrac{-\Delta H_R}{\rho C}\cdot k\big(T(t)\big)\cdot c_A(t) \\ \dfrac{d}{dt}c_A(t) = \dfrac{F}{V}\big(c_{Ai}(t) - c_A(t)\big) - k\big(T(t)\big)\cdot c_A(t) \end{cases} \tag{1}$$

where U is the overall heat transfer coefficient, A is the heat transfer area, ρ is the density, $T_i(t)$ is the temperature of the inflow, ΔH_R is the heat of reaction per mole of A that is reacted, $T_c(t)$ is the coolant temperature and $c_{Ai}(t)$ is the molar concentration of the inflow. The reaction rate constant k is a function of temperature $T(t)$ given by the Arrhenius relation

$$k\big(T(t)\big) = k_0 \exp\left(-\frac{E}{R\cdot T(t)}\right), \tag{2}$$

where k_0 is the frequency factor, E is the activation energy, and R is the gas constant. There is a strong coupling between the reactor temperature and residual concentration introduced by the product of $k(T(t))$ and $c_A(t)$ in (1). It is assumed that $c_{Ai}(t)$ and $T_i(t)$ are constants in this experiment. It is further assumed that the residual concentration $c_A(t)$ and the reactor temperature $T(t)$ are measured and available for feedback control.

The numerical values of the constants, initial conditions and parameters are listed in Table I, respectively [17].

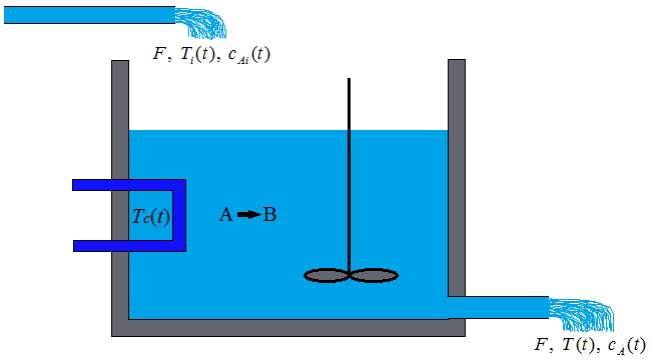

Figure 1. Continuous stirred tank reactor.

TABLE I.
Constants, Parameters and Initial conditions of CSTR

Constants	***Values (units)***	***Parameters***	***Values (units)***
F/V	1 (1/min)	E/R	5963.6 (K)
c_{Ai}	10 (kmol/m^3)	k_0	34930800 (1/min)
T_i	298.2 (K)	$\Delta H/(\rho C)$	11.92 (K·m^3/kmol)
Initial conditions	***Values (units)***	$UA/(\rho VC)$	0.3 (1/min)
$T(0)$	311.26 (K)		
$c_A(0)$	8.57 (kmol/m^3)		
$T_c(0)$	297.97 (K)		

The reactor is initially in steady-state phase with feed-in concentration c_{Ai} = 10 kmol/m^3, in-flow temperature T_i = 298.2 K, and coolant temperature $T_c(0)$ = 297.97 K, which is the manipulated variable. The initial reactor temperature $T(0)$ = 311.26 K, and the initial residual concentration $c_A(0)$ = 8.57 kmol/m^3.

Here, the intention is to transit the reaction linearly from the initial state 8.57 kmol/m^3 down to 2 kmol/m^3 in 26 minutes [17–18], which ensure slow-varying scheduling signal. During the transition, the reaction dynamics change significantly. Therefore, we linearize the nonlinear CSTR model (1) at five equally spaced equilibrium points along the desired concentration reference as in [17]. The linearization points, the associated equilibrium values, as well as the poles and DC-gains of the linearized models are collected into Table II, respectively. We have used subscript e to denote equilibrium.

Referring to Table II, the reaction is unstable at the points 2, 3 and 4, respectively. In the unstable region, the reaction must be appropriately cooled to prevent thermal runaway and overheating of the CSTR. However, the maximum rate of change of the coolant temperature T_c is limited to ±10 K/min, which restrains the achievable performance.

In the following section, we present three linearization-based control structures for adjusting the coolant temperature of the CSTR; namely, gain-scheduled cascade control, gain-scheduled model predictive control, and gain-scheduled composite nonlinear feedback control.

TABLE II.
Characterisitcs of Linearized CSTR Models at Equilibria

Linearization points, equilibrium values, poles and DC-gains			
Point number, ($c_{A,e}$)	***($T_{c,e}$, T_e)***	***Poles***	***DC-gains***
1, (8.57)	(297.98, 311.26)	–0.5225, –0.8952	(–0.0565, 0.7485)
2, (6.92)	(305.24, 327.99)	0.1733, –0.8866	(0.3326, –2.8191)
3, (5.28)	(296.79, 341.11)	0.5114, –0.8229	(0.1723, –1.3490)
4, (3.64)	(290.54, 354.72)	0.0453, –0.4991	(3.9949, –36.3997)
5, (2.00)	(305.03, 373.13)	–1.1077±j1.0901	(–0.0426, 0.6210)

III. Control System Design

Here, the intention is to design feedback control laws, which stabilize the CSTR and satisfy certain control requirements. We begin the discussion with the gain-scheduled cascade structure in Subsection A. In Subsection B, we shortly present the MPC, whereas the gain-scheduled CNF control is discussed in Subsection C. In what follows, we list the control requirements.

All control systems are required to

- follow the desired ramp reference from 8.57 kmol/m^3 to 2 kmol/m^3 in 26 minutes
- form physically realizable coolant temperature profile, which cannot vary more than ±10 K/min
- adjust the coolant temperature using sampling time T_s = 0.5 min. Hereafter, we use k to denote discrete time instant.

In addition, the residual concentration must converge to the desired final value in steady-state. The tracking performances of all control systems are measured by the IAE-criterion

$$IAE = \int_0^{t_f} |e(\tau)|\, d\tau = \int_0^{t_f} |c_{\mathrm{ref}}(\tau) - c_A(\tau)|\, d\tau\,, \qquad (3)$$

where e is the actuating error, c_{ref} is the desired residual concentration, and t_f is the stop time of the simulation.

A. Gain-Scheduled Cascade Control

Consider the block diagram of Fig. 2, which represents the well-known cascade structure. In Fig. 2, the primary loop controller is a PI-controller and the secondary loop controller is a phase-lead compensator. The coolant temperature $T_c(k)$ is adjusted using concentration and temperature measurements. However, the reaction displays significant dynamic change while the concentration is ramped down, and hence, a fixed tuning controller is unable to meet the control requirements. Therefore, the cascade controller is gain-scheduled in order to perform the control task.

The five linearized CSTR models introduced in Section 2 are used for pointwise tuning. All tuning parameter values of the cascade controller are determined using the scheduling variable dependent quadratic polynomials of the form

$$P(\mathrm{c}_A(t)) = P_0 + P_1 \cdot \mathrm{c}_A(t) + P_2 \cdot \mathrm{c}_A(t)^2\,, \qquad (4)$$

where P is a tuning parameter and $c_A(t)$ is the scheduling variable. All coefficients P_i, i = 0, 1, 2 are tunable, which are calculated based on the control requirements. To be more specific, the tuning parameters of the primary loop controller are the proportional gain K_p and the integration gain K_I, whereas K_t, a and b are the tuning parameters of the secondary loop phase-lead compensator. The scheduling variable, as an external input to the controllers, has been marked with dashed arrows into the Fig. 2, respectively.

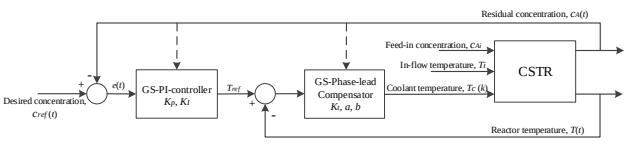

Figure 2. Gain-scheduled cascade structure.

The tunable polynomials should generally be low order in order to keep the number of tunable coefficients small. Small number of tunable coefficients keeps the calculation burden manageable. However, first-order linear polynomials are insufficient in this application because of significant nonlinearity introduced by the CSTR [17].

We follow the procedure given in [17], which results in a profile of scheduled tuning parameters depicted in Fig. 3, respectively. The individual tuning parameter values are calculated at the five distinct linearization points, which results in a collection of 25 scheduled values. Note that linear interpolation is performed between the consecutive values of each tuning parameter, which ensures that all parameters change continuously as a function of the scheduling variable. Closed-loop stability is investigated between the linearization points through simulations. Finally, the performance of the nonlinear gain-scheduled cascade controller is simulated using the nonlinear CSTR model.

The residual concentration, reactor temperature and coolant temperature obtained by the cascade controller are depicted in Fig. 4, respectively. Judging from the Fig. 4, the concentration tracking is satisfactory, and the coolant temperature changes between the given constraints. The IAE performance measure is 15.37.

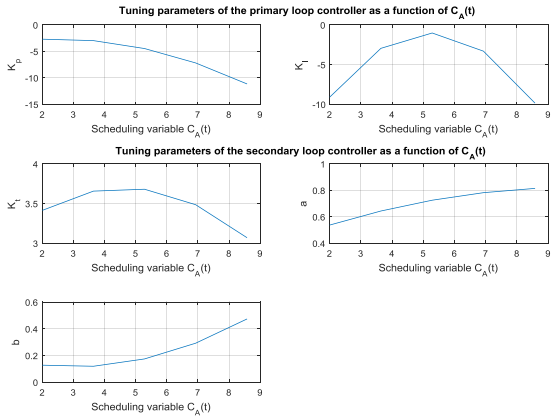

Figure 3. Tuning parameter values of the cascade controller.

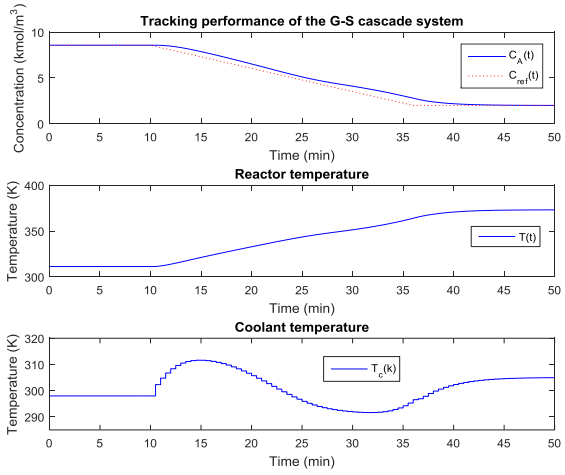

Figure 4. Residual concentration, reactor temperature and coolant temperature of the CSTR.

B. *Gain-Scheduled Model Predictive Control*

A single MPC controller designed at a specific operation point does not give satisfactory tracking performance for the entire operation range of the CSTR [18]. Therefore, multiple MPCs are designed at different operation conditions. To be more specific, three prediction models and three different MPCs are constructed in order to manipulate the coolant temperature through the transition. The MPC controllers and their prediction models are calculated offline at the preselected operation points. Also, a predefined scheduling strategy is necessary to sequence the MPCs and their prediction models while the residual concentration decreases towards the final value. Please refer to [18] for detailed discussion of the MPCs and their parameterizations.

The prediction models and MPCs are formed at [18]

A. the initial steady-state operation condition as described in Section 2

B. an intermediate operation condition, where c_A = 5.5 kmol/m^3 and T = 339 K

C. the final operation condition, where c_A = 2 kmol/m^3 and T = 373 K

The temperature values of B and C are obtained from trim analysis. Furthermore, the MPCs and the prediction models are scheduled using the following switching rules [18]

1. if $\{c_A(t) \geq 8 \text{ kmol/m}^3\}$, use the prediction model and MPC obtained at A.
2. if $\{3 \leq c_A(t) < 8 \text{ kmol/m}^3\}$, use the prediction model and MPC obtained at B.
3. if $\{c_A(t) < 3 \text{ kmol/m}^3\}$, use the prediction model and MPC obtained at C.

When the residual concentration decreases, and a new rule is executed, the dynamic character of the coolant temperature changes according to the corresponding prediction model and the MPC. However, additional transients will be generated to the coolant temperature at the switching instants.

In addition, a reference previewer has been implemented into the MPC structure, which is used to look ahead the set point changes in the future. Such previewer generally improves the set point tracking [18]. The block diagram of the gain-scheduled MPC structure is depicted in Fig. 5, respectively. The scheduler block of Fig. 5 is used to provide the switching signal for the multiple MPCs block in order to sequence suitable MPC and its prediction model according to the switching rules.

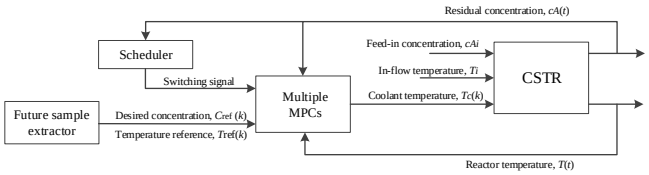

Figure 5. Gain-scheduled multiple MPC structure.

The tracking performance of the closed-loop system is depicted in Fig. 6, respectively. The switching instants have been marked onto the coolant temperature profile. The residual concentration follows the desired reference relatively closely; although, some abrupt changes are observed in the coolant temperature during switching. The IAE performance measure is 6.9.

C. *Gain-Scheduled Full-State Composite Nonlinear Feedback Control*

In this subsection, we proceed to design a gain-scheduled full-state CNF controller for adjusting the coolant temperature of the CSTR. We carry out the CNF design procedure in three steps; namely, 1) the design of linear feedback part, 2) the design of nonlinear feedback part, and 3) combine the linear and nonlinear feedback parts to form a complete CNF controller.

A full-state CNF controller can be designed with respect to linearized process dynamics described by the equations

$$\begin{cases} \dot{x} = Ax + Bu, \; x(0) = x_0 \\ y = C_y x \\ m = x \end{cases}, \tag{5}$$

where $x \in \mathbb{R}^n$, $u \in \mathbb{R}$, $y \in \mathbb{R}$ and $m \in \mathbb{R}^n$ are the state, control input, controlled output and measured output, whereas x_0 is an initial condition.

The controlled output y is assumed to be part of m, i.e. y is also measured. It is further assumed that the pair (A, B) is stabilizable, and the triple (A, B, C_y) has no invariant zeros at the origin. An integral action can be included into the design procedure by augmenting an integrator into the given system model; see for example: [11; 20]. Therefore, we insert the following auxiliary state variable

$$\dot{x}_i = r - y = -C_y x + r, \tag{6}$$

into the system (5). The resulting augmented system can then be written by

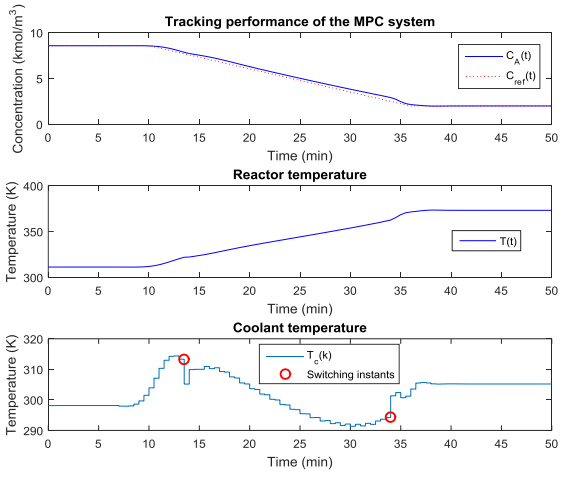

Figure 6. Tracking performance, coolant temperature, and switching instants of MPCs.

$$\begin{cases} \dot{\bar{x}} = \bar{A}\bar{x} + \bar{B}u + \bar{B}_r r,\ \bar{x}(0) = \bar{x}_0 \\ y = \bar{C}_y \bar{x} \\ \bar{m} = \bar{x} \end{cases}, \quad (7)$$

where

$$\bar{x} = \begin{bmatrix} x \\ x_i \end{bmatrix},\ \bar{x}_0 = \begin{bmatrix} x_0 \\ 0 \end{bmatrix},\ \bar{m} = \begin{bmatrix} m \\ x_i \end{bmatrix}, \quad (8)$$

and

$$\bar{A} = \begin{bmatrix} A & 0 \\ -C_y & 0 \end{bmatrix},\ \bar{B} = \begin{bmatrix} B \\ 0 \end{bmatrix},\ \bar{B}_r = \begin{bmatrix} 0 \\ 1 \end{bmatrix},\ \bar{C}_y = \begin{bmatrix} C_y & 0 \end{bmatrix}. \quad (9)$$

It can be shown that the pair $(\bar{A},\ \bar{B})$ is stabilizable. The full-state CNF controller with integration can be designed by the following three steps.

Step 1. Design a linear feedback control law

$$u_L = -K\bar{x} + R_s r, \quad (10)$$

such that $(\bar{A} - \bar{B}K)$ is asymptotically stable. The gain K can be partitioned as $K = [K_x\ \ K_i]$, where K_x is the state feedback gain and K_i is the gain of the integration action. The scalar R_s is a reference tracking gain given by

$$R_s = -[C_y (A - BK_x)^{-1} B]^{-1}, \quad (11)$$

where the inner inverse exists under the given assumptions. The gain R_s ensures that the DC-gain from the reference r to the controlled output y is one, which guarantees accurate tracking of constants in steady-state assuming disturbance free control environment. It is case dependent, when such calibration is useful, if integration action is also implemented.

Step 2. Given a positive-definite matrix $W \in \mathbb{R}^{(n+1)x(n+1)}$, solve the Lyapunov equation

$$(\bar{A} - \bar{B}K)^T P + P(\bar{A} - \bar{B}K) + W = 0 \quad (12)$$

for $P > 0$. Such solution can always be found since $(\bar{A} - \bar{B}K)$ is asymptotically stable. The nonlinear feedback law is then given by

$$u_N = \rho(r, y)\bar{B}^T P\bar{x}, \quad (13)$$

where $\rho(r,\ y)$ is any smooth nonpositive function, locally Lipschitz in y. Procedures for seeking an appropriate $\bar{B}^T P$ is presented; for example, in [11]. In this paper, we choose the following commonly-used nonlinear function

$$\rho(e) = -\beta\left|\exp(-\alpha|e|) - \exp(-\alpha|y(0) - r|)\right|,\ |e| = |r - y|, \quad (14)$$

where e is the actuating error, and $\alpha > 0$ and $\beta > 0$ are tuning parameters. The parameters α and β are chosen to give satisfactory performance when $e \to 0$. The function (14) starts from zero and converge to

$$\rho_0 = -\beta\left|1 - \exp\left(-\alpha|y(0) - r|\right)\right| \quad (15)$$

with appropriate speed and magnitude, while $e \to 0$. The parameter α is selected to yield sufficient convergence speed, whereas β is selected to give a desired magnitude in steady-state. It is usually relatively simple to find suitable values for α and β following few practical experiments or using simulations. However, several additional ways to tune the nonlinear function is discussed in [7], respectively. In this paper, we use fixed tunings for α and β.

Step 3. Form the full CNF control law by combining the linear and nonlinear feedback laws from the previous steps:

$$u = u_L + u_N = -K\bar{x} + R_s r + \rho(r, y)\bar{B}^T P\bar{x}. \quad (16)$$

The proof of the asymptotic stability of the closed-loop system under such control law can be found; for example, in [11].

We begin the CNF design from the step 1. First, we calculate a collection of state feedback gains K_x using the well-known LQR methodology at the points 1–5 of Table II. To be more specific, we tune the gains K_x by minimizing the infinite horizon LQR cost function

$$J_{lqr} = \int_0^\infty (x^T Qx + u^T Ru)dt, \quad (17)$$

where $Q \in \mathbb{R}^{2x2} \geq 0$, $R \in \mathbb{R} > 0$ in this application. We choose the weighting matrix $Q = I^{2x2}$, because the dynamic behavior of the reactor temperature and residual concentration are essentially the same. The weighting factor $R = 0.1$ was found experimentally to keep the gains at a reasonable magnitude, and hence, to ensure unviolated rate-limit constraint.

The resulting feedback gains are collected in Table III, respectively. Furthermore, we choose a fixed integration gain $K_i = -6$. Our initial simulation tryouts suggested that the gains at the first node should be retuned in order to accelerate the reaction at the beginning of the ramp, i.e. the initial LQR tuning was too conservative. We updated the gain of the first node by placing the poles at $[-1.5 \pm j0.4]$ in the complex plane. Such fine-tuning results in the gain $K_{x,1} = [-3.6319,\ 5.2746]$, where the lower index 1 indicates the first design node, i.e. the first linearization point.

Finally, we linearly interpolate between the gain values, and we use gain-scheduling to update the gains K_x using $c_A(t)$ as a slowly varying scheduling variable. As a result, the state feedback gains $K_x(c_A(t))$ change continuously while the residual concentration decreases towards the desired value.

Next, we solve the Lyapunov equation (12) with $W = I^{3x3}$, which results in a well-conditioned P given by

TABLE III.
LINEARIZATION POINTS AND LQR GAINS

Point number, (cA)	***Kx***
1, (8.57)	(1.9668, 2.2535)
2, (6.92)	(9.5570, 4.6862)
3, (5.28)	(21.9479, 6.8175)
4, (3.64)	(33.7653, 6.9147)
5, (2.00)	(29.8291, 3.9893)

$$P=\begin{bmatrix}43.8237 & 5.5578 & 3.3592\\ 5.5578 & 0.8845 & -0.2778\\ 3.3592 & -0.2778 & 17.5506\end{bmatrix}>0,\ P=P^T. \quad (18)$$

Therefore, we use fixed tuning for the gains $\bar{B}^T P$ at the entire operation region. The resulting gains for the nonlinear part are

$$\bar{B}^T P=[1.6673 \quad 0.2654 \quad -0.0833]. \quad (19)$$

We choose the fixed parameters of the nonlinear function (14) as α = 3 and β = 1, which completes the CNF design. The resulting state-error CNF controller is

$$\begin{aligned}T_c(t)&=u(t)=u_L(t)+u_N(t)=-K\cdot\bar{x}(t)+\rho(e)\bar{B}^T P\cdot\bar{x}(t)\\&=[-K_x(c_A(t)) \ -6]\cdot\bar{x}(t)\\&+\rho(e(t))\cdot[1.6673 \quad 0.2654 \quad -0.0833]\cdot\bar{x}(t),\end{aligned}$$

$$\rho(e(t))=-1\left|\exp(-3|e(t)|-\exp(-3|c_A(0)-c_{\text{ref}}(t)|)\right|,$$

$$\bar{x}(t)=\begin{bmatrix}c_{\text{ref}}(t)-c_A(t)\\ T_{\text{ref}}(t)-T(t)\\ x_i(t)\end{bmatrix},\ |e(t)|=|c_{\text{ref}}(t)-c_A(t)|,$$

$$x_i(t)=\int_0^{t_f}\left(c_{\text{ref}}(\tau)-c_A(\tau)\right)d\tau, \quad (20)$$

where $T_{\text{ref}}(t)$ is the desired reactor temperature.

Finally, for simulation purpose, we discretize the control law (20) using the zero-order hold method. The block diagram of the gain-scheduled full-state CNF controller is depicted in Fig. 7, respectively. In Fig. 7, the scheduler block provides the LQR state feedback gains to the CNF controller.

We have implemented the scheduler block using one dimensional MatLab lookup table, in which the breakpoints are the five linearization points of Table II. The total number of scheduled gain values are 10, which is less compared with the cascade structure in Subsection A. However, the CNF controller has additional fixed gains and tuning parameters; namely, $\bar{B}^T P$, K_i, α and β. Therefore, the CNF has more tuning parameters compared with the cascade controller, and hence, more freedom available for controller tuning.

The desired temperature of Fig. 7 is provided by the temperature generator block. We have calculated pointwise model-based temperature values at each design node using information from trim analysis. Then we linearly interpolate between the calculated values using one dimensional MatLab lookup table, which is driven by the reference $c_{\text{ref}}(t)$. As a result, we obtain a continuous desired temperature profile to supplement the CNF controller.

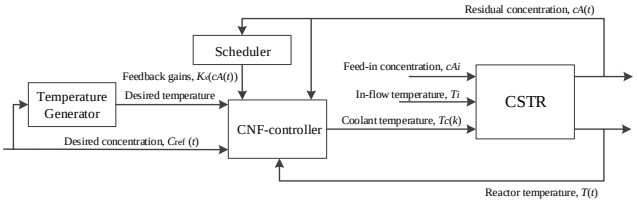

Figure 7. Gain-scheduled full-state CNF structure with temperature generator.

The closed-loop tracking performance obtained by the gain-scheduled CNF controller is depicted in Fig. 8. Judging from Fig. 8, the residual concentration follows the desired reference with marginal error only. We would like to emphasize that the nonlinear part of the CNF is fully activated when e becomes small. The role of the nonlinear part in such circumstances is to provide significant control contribution, which allow improved tracking performance and small error. The IAE index is 4.4. Finally, we collect the IAE performance measures of all control systems into Fig. 9, respectively.

The gain-scheduled CNF yields the smallest IAE number compared with the other two candidates. We also tried scheduling strategy for the gains $\bar{B}^T P$ by designing a different P at each design node. However, we did not observe significant improvement of the responses. We believe that scheduling of the gains of the nonlinear part is unnecessary in this application, because the nonlinear function (14) is able to automatically change its value using information of the error only, and hence, it is able to provide necessary fine tuning.

The gain-scheduled cascade controller resulted in worse tracking performance compared with the gain-scheduled CNF. The CNF and cascade controllers explicitly adjust the coolant temperature using information from the concentration error: $c_{\text{ref}} - c_A$, and temperature error: $T_{\text{ref}} - T$, respectively. However, the CNF has an additional tunable, error dependent nonlinear function, which is able to smoothly and automatically change the tuning of the nonlinear part as desired. Therefore, the CNF also has more structural freedom to generate feedback control compared with the traditional cascade structure. We believe that such structure-wise difference explains the superiority of the CNF.

All systems simulated in this paper used concentration and temperature measurements to generate feedback control. However, it is relatively uncommon that the residual concentration is measured in an actual reactor. We feel that estimation of the residual concentration should not be too difficult by a state observer. Therefore, an observer-based control strategy should be possible to construct for this application.

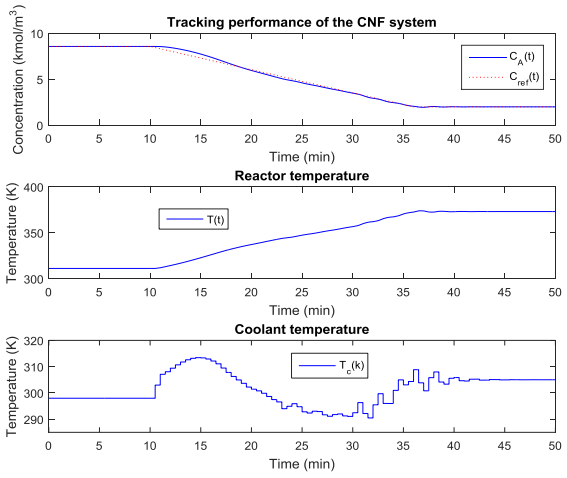

Figure 8. Performance of the closed-loop CSTR using CNF controller.

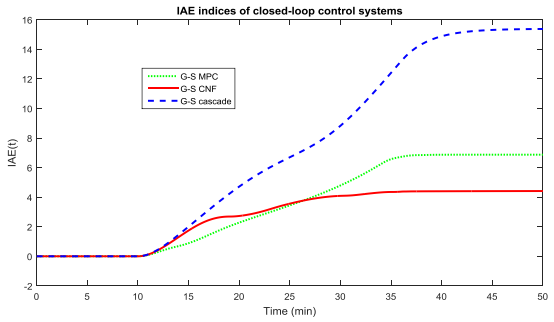

Figure 9. IAE performance measures.

IV. Concluding Remarks

Linearization-based gain-scheduled composite nonlinear feedback control was introduced in this paper. A nonlinear continuous stirred tank reactor transitioning from high to low residual concentration was used as a benchmark process to illustrate controller performance. The tracking performance of the gain-scheduled CNF was compared with a linearization-based gain-scheduled cascade controller, as well as with a linearization-based gain-scheduled model predictive controller using the well-known IAE criterion.

It was shown by simulation that the closed-loop system using the gain-scheduled CNF controller provided the best tracking performance. However, analytical approaches to investigate stability and performance properties of gain-scheduled CNF should be addressed to supplement extensive numerical simulations. Also, linear parameter-varying (LPV) and linear fractional transformation (LFT) based gain-scheduling approaches exist, which could be suitable for the CNF methodology. We feel that those could be interesting research topics in the future.

Acknowledgment

We would like to thank anonymous reviewers for their insightful comments, which helped us to improve the quality and technical merit of our paper.

References

[1] Z. Lin, M. Pachter, and S. Banda, "Toward improvement of tracking performance – nonlinear feedback for linear systems," *Int. J. Control*, vol. 70, pp. 1–11, Nov. 1998.

[2] M.C. Turner, I. Postlethwaite, and D.J. Walker, "Nonlinear tracking control for multivariable constrained input linear systems," *Int. J. Control*, vol. 73, pp. 1160–1172, Aug. 2000.

[3] B.M. Chen, T.H. Lee, K. Peng, and V. Venkataramanan, "Composite nonlinear feedback control for linear systems with input saturation: theory and an application," *IEEE Trans. Autom. Control*, vol. 48, pp. 427–439, Mar. 2003.

[4] Y. He, B.M. Chen, and C. Wu, "Composite nonlinear control with state and measurement feedback for general multivariable systems with input saturation," *Syst. Contr. Lett.*, vol. 54, pp. 455–469, May 2005.

[5] W. Lan, B.M. Chen, and Y. He, "On improvement of transient performance in tracking control for a class of nonlinear systems with input saturation," *Syst. Contr. Lett.*, vol. 55, pp. 132–138, Feb. 2006.

[6] V. Venkataramanan, K. Peng, B.M. Chen, and T.H. Lee, "Discrete-time composite nonlinear feedback control with an application in design of a hard disk drive servo system," *IEEE Trans. Contr. Syst. Technol.*, vol. 11, pp. 16–23, Jan. 2003.

[7] W. Lan, C.K. Thum, and B.M. Chen, "A hard disk drive servo system design using composite nonlinear feedback control with optimal nonlinear gain tuning methods," *IEEE Trans. on Ind. Electron.*, vol. 57, pp. 1735–1745, Sep. 2010.

[8] G. Cheng, K. Peng, B.M. Chen, and T.H. Lee, "Improving transient performance in tracking general references using composite nonlinear feedback control and its application to high-speed XY-table positioning mechanism," *IEEE Trans. Ind. Electron.*, vol. 54, pp. 1039–1051, Apr. 2007.

[9] V.-P. Pyrhonen and H. J. Koivisto, "On improvement of transient stage of composite nonlinear feedback control using arbitrary order set point filters," in Proc. *4th IEEE International Conference on Control System, Computing and Engineering*, Penang, Malaysia, Nov. 2014, pp. 147–152.

[10] G. Cai, B.M. Chen, K. Peng, and M. Dong, "Modeling and control of the yaw channel of a UAV helicopter," *IEEE Trans. Ind. Electron.*, vol. 5, pp. 3426–3434, Sep. 2008.

[11] B.M. Chen, T.H. Lee, K. Peng, and V. Venkataramanan, *Hard disk drive servo systems*, 2nd ed., Springer, New York, 2006, ch. 5.

[12] G. Cheng, and K. Peng, "Robust composite nonlinear feedback control with application to a servo positioning system," *IEEE Trans. Ind. Electron.*, vol. 54, pp.1132–1140, Apr. 2007.

[13] W. Lan and Q. Zhou, "Speed control of DC motor using composite nonlinear feedback control," in *Proc. IEEE Conf. on Control and Automation*, Christchurch, New Zealand, Dec. 2009, pp. 2160–2164.

[14] X. Yu and W. Lan, "Optimal composite nonlinear feedback control for a gantry crane system," in *Proc. 31st Chinese Control Conference*, Hefei, China, July 2012, pp. 601–606.

[15] S. Erzen, M. Pahlevaninezhad, A. Bakhshai, and P.K. Jain, "Composite nonlinear feedback control and stability analysis of a grid-connected voltage source inverter with LCL filter," *IEEE Trans. Ind. Electron.* vol. 60, pp. 5059–5074, Nov. 2013.

[16] L. Wei, F. Fang, and Y. Shi, "Adaptive backstepping-based composite nonlinear feedback water level control for the nuclear U-tube steam generator," *IEEE Trans. Contr. Syst. Technol.*, vol. 22, pp. 369–377, Jan. 2014.

[17] MathWorks MatLab documentation, "Gain-scheduled control of a chemical reactor," in MathWorks MatLab Release 20015a, 2015.

[18] MathWorks MatLab documentation, "Gain-scheduled MPC control of nonlinear chemical reaction," in MathWorks MatLab Release 20015a, 2015.

[19] D.E. Seborg , T.F. Edgar, and D. A. Mellichamp, *Process Dynamics and Control*, 2nd ed., Wiley, 2004, pp. 34–36.

[20] K. Peng, B.M. Chen, G. Cheng, and T.H. Lee, "Modeling and compensation of nonlinearities and friction in a micro hard disk drive servo system with nonlinear feedback," *IEEE Trans. Contr. Syst. Technol.*, vol. 13, pp. 708–721, Sep. 2005.